Biogeosciences Discuss., 12, 7209–7255, 2015
www.biogeosciences-discuss.net/12/7209/2015/
doi:10.5194/bgd-12-7209-2015

Biogeosciences Discussions
Open Access

Effects of nitrate and phosphate supply on chromophoric and fluorescent dissolved organic matter in the Eastern Tropical North Atlantic: a mesocosm study

A. N. Loginova, C. Borchard, J. Meyer, H. Hauss, R. Kiko, and A. Engel

GEOMAR Helmholtz-Centre for Ocean Research Kiel, Düsternbrooker Weg 20, 24105 Kiel, Germany

Received: 24 April 2015 – Accepted: 24 April 2015 – Published: 18 May 2015

Correspondence to: A. N. Loginova (aloginova@geomar.de)

Published by Copernicus Publications on behalf of the European Geosciences Union.

Abstract

The Eastern Tropical North Atlantic (ETNA) is an open ocean region with little input of terrestrial dissolved organic matter (DOM), suggesting that pelagic production has to be the main source of DOM. Inorganic nitrogen (DIN) and phosphorus (DIP) concentrations affect pelagic production, leading to DOM modifications. The quantitative and qualitative changes in DOM are often estimated by its optical properties. Colored DOM (CDOM) is often used to estimate dissolved organic carbon (DOC) concentrations by applied techniques, e.g. through remote sensing, whereas DOM properties, such as molecular weight, can be estimated from the slopes of the CDOM absorption spectra (S). Fluorescence properties of CDOM (FDOM) allow discriminating between different structural CDOM properties. The investigation of distribution and cycling of CDOM and FDOM was recognized to be important for understanding of physical and biogeochemical processes, influencing DOM. However, little information is available about effects of nutrient variability on CDOM and FDOM dynamics. Here we present results from two mesocosm experiments conducted with a natural plankton community of the ETNA, where effects of DIP ("Varied P") and DIN ("Varied N") supply on optical properties of DOM were studied. CDOM accumulated proportionally to phytoplankton biomass during the experiments. S decreased over time indicating accumulation of high molecular weight DOM. In Varied N, an additional CDOM portion, as a result of bacterial DOM reworking, was determined. It increased the CDOM fraction in DOC proportionally to the supplied DIN. The humic-like FDOM component (Comp.1) was derived by bacteria proportionally to DIN supply. The bound-to-protein amino acid-like FDOM component (Comp.2) was released irrespectively to phytoplankton biomass, but depending on DIP and DIN concentrations, as a part of an overflow mechanism. Under high DIN supply, Comp.2 was removed by bacterial reworking processes, leading to an accumulation of humic-like Comp.1. No influence of nutrient availability on amino acid-like FDOM component in peptide form (Comp.3) was observed. Comp.3 potentially acted as an intermediate product during formation or degradation Comp.2. Our findings suggest that

BGD
12, 7209–7255, 2015

changes in nutrient concentrations may lead to substantial responses in the quantity and "quality" of optically active DOM and, therefore, might bias results of the applied techniques for an estimation of DOC concentrations in open ocean regions.

1 Introduction

Dissolved organic matter (DOM) is the largest dynamic pool of organic carbon in the ocean. Its global inventory constitutes of approximately 662 pentagrams of carbon (PgC) (Hansell et al., 2009). Labile and semi-labile high molecular weight (HMW) DOM is released primarily by phytoplankton (Carlson and Hansell, 2015). It is used as substrate by the heterotrophic communities, which, in turn, release less bioavailable semi-refractory or even refractory DOM, thereby modifying the quantity and quality of the DOM pool (Azam et al., 1983; Ogawa et al., 2001; Jiao et al., 2010). Therefore, oceanic DOM is a complex mixture of organic compounds with different characteristics, such as molecular structure and molecular weight, resulting in different optical properties (Stedmon and Nelson, 2015).

For instance, the presence of conjugated double bonds (polyenes) results in the absorption of light in the UV and visible wavelength ranges (Stedmon and Álvarez-Salgado, 2011). The light absorbing DOM fraction is referred to as "chromophoric" or "colored" DOM (CDOM) (Coble, 2007). Due to its abilities to absorb in a wide wavelength range, CDOM may protect primary producers from harmful UV irradiation in the water column, but may also reduce photosyntetically active radiation as it absorbs at chlorophyll absorption maxima (Zepp et al., 2008). Photons absorbed by CDOM induce the formation of free radicals, which by colliding with other molecules or other radicals produce new organic molecules, reducing metals or introducing short inorganic and organic substances as byproducts (Sulzberger and Durisch-Kaiser, 2008). Modified by photoreactions, CDOM may serve as biological substrates for auto- and heterotrophic communities, releasing nutrients and low molecular weight (LMW) organic compounds,

BGD
12, 7209–7255, 2015

as well as a source of trace gases (e.g. CO, CO_2) (Kieber et al., 1990; Moran and Zepp, 1997; Kieber et al., 1999).

CDOM absorption has often been used as an indicator for DOC concentrations in the Ocean (Fichot and Benner, 2011, 2012; Rochelle-Newall et al., 2014). For example, DOC concentration in estuarine surface waters can be derived from CDOM absorption by remote sensing techniques, assuming a direct relationship between CDOM absorption and DOC concentrations (Del Castillo, 2005). In the open ocean, however, this relationship varies throughout the water column (Nelson and Siegel, 2013), and factors affecting it are poorly understood.

A better knowledge on factors influencing the CDOM/DOC relationship could improve our understanding of DOM cycling, as well as of the regulation of light attenuation in the ocean. Furthermore, the knowledge of the factors, influencing the open ocean CDOM/DOC relationship would be useful for the estimation of DOC concentrations from CDOM absorption measurements by remote sensing techniques.

As CDOM embodies a complex mixture of organic compounds that have overlapping absorption spectra, with, generally, no single compound dominating (Del Vecchio and Blough, 2004), CDOM absorbance spectra generally decrease exponentially toward longer wavelength, with no discernible peaks. Therefore, the CDOM concentration is commonly expressed as absorption coefficient at chosen wavelength (e.g. 325, 355, 375 nm) (Stedmon et al., 2001; Fichot and Benner, 2012; Nelson and Siegel, 2013).

To derive information on CDOM quality, such as molecular weight and modification processes, spectral slopes of CDOM light absorption and spectral slopes ratio are used (Helms et al., 2008; Zhang et al., 2009).

It has been shown that spectral slopes at wavelength regions 275–295 nm and 300–500 nm ($S_{275–295}$ and $S_{300–500}$) decrease with increasing in DOM molecular weight, and, therefore, may be used as an indicator of accumulation/degradation of bioavailable HMW-DOM (De Haan and De Boer, 1987; Helms et al., 2008; Zhang et al., 2009).

The ratio of $S_{275–295}$ to spectral slope at wavelength region 350–400 nm ($S_{350–400}$), S_R, is used to estimate CDOM transformations. S_R increases as CDOM becomes

BGD
12, 7209–7255, 2015

involved in photoreactions and decreases as CDOM is microbially reworked (Helms et al., 2008).

The presence of aromatic rings in CDOM often also results in fluorescence (Stedmon and Álvarez-Salgado, 2011).

Fluorescent DOM (FDOM) excitation/emission (Ex/Em) spectra allow discriminating between different pools of CDOM (Coble, 2007; Stedmon and Bro, 2008; Mopper et al., 2007; Yamashita et al., 2010). The substances that are excited and emit in the UV spectral range commonly correspond to labile proteinaceous DOM, and therefore are referred to as amino acid-like (tyrosine- and tryptophan-like) FDOM (e.g. Coble, 1996). The substances that are excited in the UV spectral range, but emit in the visible spectral range were identified as fulvic- and humic-like FDOM (Gueguen and Kowalczuk, 2013). Tyrosine- and Tryptophan-like substances have been used for the assessment of in situ primary productivity, while humic-like substances are used for the indication of allochtonous (e.g. riverine) DOM or microbial DOM transformation (Coble, 1996).

Although the CDOM and FDOM distribution and cycling has been described for many open ocean sites (Nelson and Siegel, 2013; Jorgensen et al., 2011), specific sources and factors influencing their composition and transformations are yet not well understood.

For example, CDOM accumulation is often related to nutrient remineralization (Swan et al., 2009; Nelson and Siegel, 2013). However, the effects of nutrient variability on CDOM concentration and on the relationship between CDOM and DOC are largely understudied.

Stedmon and Markager (2005) have reported that nutrients affect freshly produced marine FDOM pools in an Arctic fjord system. In their study, the amino acid-like fluorescence was enhanced under phosphate and silica limitation, but was independent from phytoplankton composition. Bacterially produced humic-like FDOM components were reported to accumulate under phosphate and silica limitation as well. However, the authors revealed some doubts about a setup of phosphorus limitation. Therefore, the influence of inorganic nutrients on FDOM components remains to be resolved.

BGD
12, 7209–7255, 2015

As the Eastern Tropical North Atlantic (ETNA) is an open ocean region with, supposedly, little terrestrial DOM input, DOM has to be mainly produced by pelagic production.

In classical view, the ETNA is considered as an "excess nitrogen (N)" region compared to the "Redfield N : P ratio" of 16 (see Redfield, 1987 and Gruber and Sarmento, 1997) reflecting high rates of biological N-fixation due to Saharan dust deposition, with N : P ratios 16–25 at depth (see Fanning, 1992). It features a shallow OMZ at about 100 m depth (Brandt et al., 2015) and a deeper OMZ at approximately 300–500 m depth with oxygen concentrations up to 40 µmol kg^{-1} (Karstensen et al., 2008). However, eddies originating in the Mauritanian upwelling regime and propagating westward can harbor much lower oxygen concentrations (~ 4 µmol O_2 kg^{-1}; Karstensen et al., 2014), potentially enabling N-loss processes (Strous et al., 2006; Kartal et al., 2007; Jetten et al., 2009; Jayakumar et al., 2009). Those mesoscale eddies, may support nutrient loaded but relatively N deficient waters to the surface (McGillicudy et al., 2003, 2007; Mathis et al., 2007). Furthermore, it has been shown that non-diazotroph primary production in the ETNA can be N-limited (Franz et al., 2012; Hauss et al., 2013).

Here we investigated the effects of different DIN and dissolved inorganic phosphorous (DIP) concentrations and of their supply ratio (DIN : DIP) on DOM "quality" by using spectroscopic methods of DOM analysis (e.g. accumulation and properties of CDOM and FDOM) during mesocosm experiments with natural pelagic communities of the Cape Verdean Archipelago, an area, affected by low oxygen-core eddies.

During these mesocosm experiments, we tested whether (1) pelagic production is a source of CDOM and FDOM, (2) CDOM and FDOM accumulation and composition are affected by changes in nutrient stoichiometry, and whether (3) the relationship between CDOM absorption and DOC concentrations is stable under variable nutrient concentrations.

To do so, DOC concentrations, CDOM absorption and CDOM properties ($S_{275–295}$ and S_R), FDOM fluorescence, as well as chlorophyll *a* (chl *a*), and bacterial abundance, were analyzed during the course of two mesocosm experiments, conducted as

BGD
12, 7209–7255, 2015

a part of the Collaborative Research Centre 754 (SFB754) “Climate–Biogeochemistry Interactions in the Tropical Ocean” (www.sfb754.de).

2 Methods

2.1 Setup of the mesocosms experiment

Two 8-day mesocosm experiments were conducted consecutively in October 2012 at the Instituto Nacional de Desenvolvimento das Pescas (INDP), Mindelo, Cape Verde. Seawater from 5 m depth was collected into four 600 L tanks in the night of the 1 to 2 Ocotber and 11 to 12 October for the first and second experiment, respectively. The sampling was done with the RV *Islândia* south of São Vicente (16°44.4′ N, 25°09.4′ W). For each experiment, sixteen mesocosm-bags were placed floating in 4 cooling baths that were kept at surface seawater temperature (25.9–28.7 °C) using “flow-through” principle with the water from the Mindelo bay in front of the INDP. The mesocosms were filled alternately (about 10 s per filling event) and randomly from the tanks by gravity flow using submerged hose in order to achieve even distribution of the water and minimize bubble formation. A mesh to filter zooplankton was not used. The precise volume of each mesocosm was determined by addition of 1.5 mmol of silicate and subsequent measurement of the resulting silicate concentration. The water volume in the mesocosms ranged from 106 to 145 L. For simulation of surface water conditions, the mesocosms were shaded with blue transparent lids to approximately 20 % of sunlit irradiation (56–420 $\mu E\,m^{-2}\,s^{-1}$, depending on cloud cover).

Nutrients were manipulated by adding different amounts of phosphate (DIP) and nitrate (DIN). In the first experiment, the DIP supply was varied (Varied P) at relatively constant DIN concentrations in twelve of the sixteen mesocosms, while in the second experiment the initial DIN concentrations were varied (Varied N) at constant DIP supply in twelve of the sixteen mesocosms.

BGD
12, 7209–7255, 2015

In addition to this, four "cornerpoints", where both, DIN and DIP, were varied, were chosen to be repeated during both experiments (see target DIN and DIP values in Table 1). However, during the first experiment, setting the nutrient levels in one of the "cornerpoint" mesocosms (mesocosm 10) was not successful and it was decided to adjust the DIN- and DIP-concentrations in this mesocosm to "Redfield N : P ratio" of 16 (Redfield, 1987) and therefore add another replicate to the treatment 12.00N/0.75P. Another "cornerpoint" mesocosm (mesocosm 5) during the first experiment was excluded from further analyses as no algal bloom had developed.

Initial sampling for biogeochemical parameters was accomplished immediately after the mesocosms filling (day 1). Nutrients were added after the initial sampling. Further water sampling was conducted daily between 9 and 10.30 a.m. on days 2 to 8.

The target and actual nutrient concentrations are shown in Table 1 and the corresponding treatment indications will be used in the following.

2.2 Sampling and analyses

2.2.1 Particulate organic matter

Samples of 0.5 L for chl *a* measurements were vacuum-filtered (< 200 mbar) onto Whatman GF/F filters (25 mm, 0.7 µm), 1 mL of ultrapure water was added and the filters were frozen at −20 °C for at least 24 h. Subsequently, pigments were extracted using acetone and measured in a Trilogy® fluorometer (Turner Designs) calibrated with a chl *a* standard (Anacystis nidulans, Walter CMP, Kiel, Germany) dilution series (Parsons et al., 1984).

For bacterial cell counts, samples (5 mL) were fixed with 2 % formaldehyde, frozen at −80 °C and transported to the home laboratory. Samples were diluted 1 : 3, stained with SYBR-Green and measured at a flow rate of 11.0 µL min^{-1} by flow cytometry (FACScalibur, Becton Dickinson, San Jose, CA, USA).

BGD
12, 7209–7255, 2015

2.2.2 Dissolved organic matter

Dissolved organic carbon (DOC) duplicate samples (20 mL) were filtered through combusted GF/F filters and collected in combusted glass ampoules. Samples were acidified with 80 µL of 85 % phosphoric acid, flame sealed and stored at 4 °C in the dark until analysis.

DOC samples were analysed by applying the high-temperature catalytic oxidation method (TOC-VCSH, Shimadzu) after Sugimura and Suzuki (1998). The instrument was calibrated every 8–10 days by measuring of 6 standard solutions of 0, 500, 1000, 1500, 2500 and 5000 µg C L^{-1}, prepared using a potassium hydrogen phthalate standard (Merck 109017). Every day before each set of measurements, ultrapure (MilliQ) water was used for setting the instrument baseline, following by the measurement of the deep-sea water standard (Hansell, 2005) with known DOC concentration in order to verify result representation by the instrument. Additionally, two DOC control samples were prepared each day of measurement using a potassium hydrogen phthalate standard (Merck 109017). The control samples had dissolved carbon concentrations within the range of those in samples and were measured along the sample analyses in order to avoid mistakes due to baseline flow during measurements. The DOC concentration was determined in each sample out of 5 to 8 replicate injections.

For chromophoric dissolved organic matter (CDOM) and fluorescent dissolved organic matter (FDOM), 2 × 35 mL samples for each parameter were collected daily into combusted (450 °C, 8 h) amber-glass vials after filtering through 0.45 µm polyethersulfone syringe filters (CHROMAPHIL® Xtra PES-45/25, MACHEREY-NAGEL GmbH & Co.KG). The samples were stored at 4 °C in the dark during 6 month pending analyses. All samples were brought to room temperature before analyses.

Absorption of chromophoric dissolved organic matter (CDOM) was detected using a 100 cm path length liquid waveguide cell (LWCC-2100, World Precision Instruments, Sarasota, Florida) and a UV-VIS spectrophotometer (Ocean Optics USB 4000) in con-

BGD
12, 7209–7255, 2015

junction with the Ocean Optics DT-MINI-CS light source. The absorbance was measured relatively to ultrapure water (MilliQ) by injection to the cell with a peristaltic pump.

For the determination of fluorescent dissolved organic matter (FDOM), 3-D fluorescence spectroscopy – Excitation-Emission Matrix Spectroscopy (EEMs) – was performed using a Cary Eclipse Fluorescence Spectrophotometer (Agilent Technologies) equipped with a xenon flash lamp. The fluorescence spectra for samples were measured in a 4-optical window 1 cm Quartz SUPRASIL® precision cell (Hellma® Analytics). The blank-3-D fluorescence spectra and Water Raman scans were performed daily using an Ultra-Pure Water Standard sealed cuvette (3/Q/10/WATER; Starna Scientific Ltd). The experimental wavelength range for sample and ultra-pure water scans was 230 to 455 nm in 5 nm intervals on excitation and 290 to 700 nm in 2 nm intervals on emission. Water Raman scans were recorded from 285 to 450 nm at 1 nm intervals for emission at the 275 nm excitation wavelength (Murphy et al., 2013). All fluorescence measurements were managed at 19 °C (Cary Single Cell Peltier Accessory, VARIAN), PMT 900V, 0.2 s integration times and 5 nm slit width on excitation and emission monochromators. The absorbance for EEMs corrections was procured simultaneously with Shimadzu® 1800 UV-VIS double-beam spectrophotometer. The absorbance was measured at the room temperature (~ 19 °C) in 2-optical window 5 cm Quartz SUPRASIL® precision cell (Hellma® Analytics). The measurements were done at 1 nm wavelengths intervals from 230 to 750 nm against MilliQ water as a reference. The obtained data were converted to absorbance in a 1 cm cell.

2.3 Data evaluation

2.3.1 CDOM

The measured CDOM absorbance spectra were corrected to the refractive index of remaining particulate matter and colloids after Zhang et al. (2009) and for salinity after Nelson et al. (2007), and converted to absorption coefficients according to Bricaud

BGD
12, 7209–7255, 2015

et al. (1981):

$$a_\lambda = 2.303A(\lambda)/L; \quad (1)$$

where a_λ – is the absorption coefficient at wavelength λ (m^{-1}), $A(\lambda)$ – is the absorbance value at same wavelength and L – is the effective optical path length (m).

Commonly, absorption coefficients at 355 (a_{355}) and 375 (a_{375}) nm are used to express CDOM concentrations in coastal waters (Granskog et al., 2007; Stedmon et al., 2011), since CDOM concentrations there are very high, and absorption coefficient at 440–445 nm (a_{440}) is used for comparison of field CDOM measurements to remote sensing (Swan et al., 2013).

Open ocean waters show only very low absorbance at wavelengths of 400–600 nm. Therefore, absorption at 325 nm (a_{325}) is often used for expression of the open ocean CDOM concentrations (Nelson and Siegel, 2013).

The area off Cape Verdean Archipelago, where water for mesocosms was taken, is not influenced by river inflow and is considered as the open ocean area. Thus, a_{325} was chosen for expression of CDOM concentration. For comparison of CDOM properties with models developed previously a_{355} and a_{375} were obtained, as well.

No universal wavelength range or method is used in the literature for calculation of CDOM spectral slopes (S). Instead, S is often calculated by nonlinear least square fitting for relatively long wavelength ranges and by log-transformed linear regression for shorter wavelength ranges (Twardowski et al., 2004; Helms et al., 2008). Both, nonlinear fitting and log-transformed linear regression, as well as several wavelength ranges, were used in this work for estimation of CDOM properties and their comparison to the literature.

The spectral slope for the interval 320–500 nm (S_{SEMO}) was determined by fitting the absorption spectra to the simple exponential model with offset (SEMO; Twardowski et al., 2004) using nonlinear least square fitting (MATLAB, The MathWorks Inc.). This model was chosen as it explained best the shape of CDOM absorption spectra, ob-

BGD
12, 7209–7255, 2015

tained in our study, in the given wavelength range from all nonlinear models tested after Twardowski et al. (2004).

Spectral slopes for the intervals 275–295 nm ($S_{275–295}$) and 350–400 ($S_{350–400}$) were calculated after Helms et al. (2008) using log-transform linear regression.

The CDOM alteration indicator, slope ratio (S_R), was calculated after Helms et al. (2008) as well, as ratio of $S_{275–295}$ to $S_{350–400}$.

To describe the CDOM properties the following equation was used:

$$S_{SEMO} = \alpha + \beta / a_{375}; \quad (2)$$

where α and β are the regression coefficients. The properties were compared to the model of Stedmon and Markager (2001) for marine CDOM developed for the Greenland Sea, in which $\alpha = 7.4$ and $\beta = 1.1$.

The variability of the relationship a_{355}/DOC vs. $S_{275–295}$ was compared with the model developed by Fichot and Benner (2012) for DOC calculation from known a_{355} and $S_{275–295}$:

$$a_{355}/\mathrm{DOC} = e^{(\gamma - \delta S_{275–295})} + e^{(\varepsilon - \zeta S_{275–295})}; \quad (3)$$

where $\gamma = 5.679$, $\delta = 81.299$, $\varepsilon = 8.459$ and $\zeta = 241.052$ are regression coefficients developed for the river estuaries (after Fichot and Benner, 2012).

2.3.2 FDOM

The 3-D fluorescence spectra were corrected for spectral bias, background signals and inner filter effects. Each EEM was normalized to the area of the ultra-pure water Raman peaks, measured in the same day. EEMs were combined into three-dimensional data array, analyzed by PARAFAC (Stedmon and Bro, 2008) and validated by split-half analysis using "drEEM toolbox for MATLAB" after Murphy et al. (2013).

Only up to 3-components could be validated. For models with more than 3 components the results varied during split-half analysis (see Murphy et al., 2013), indicating

BGD
12, 7209–7255, 2015

the possibility of identifying the instrument noise as a signal (e.g. Stedmon and Markager, 2005). The fluorescence of each component is stated as fluorescence at excitation and emission maximums in Raman units (RU). The spectral characteristics of these components are described in Table 3.

2.3.3 Mesocosm data treatment

Based on the nutrient component that was mainly varied, the experiments are referred to as Varied P and Varied N in the following.

High variability of CDOM components (Fig. S1) was observed on day 1 and day 2 of Varied P and day1 of Varied N. This variability was likely associated to the filling and manipulation of the mesocosm bags and vanished afterwards. These days were excluded from further calculations, and day 3 and day 2 were defined as "start" or "beginning" of Varied P and Varied N, respectively. Day 8 was defined as the "end" of both experiments. To exclude initial variability, changes of the different DOM parameters over time were calculated as the difference between sampling day and start day:

$$\Delta Ci(k) = Ci(k) - Ci(\text{start}); \quad (4)$$

where C is a concentration, absorption or fluorescence intensity, i is a mesocosm id (i = 1–16) and k is the day of experiment.

For the presentation of the development over time, POM and ΔDOM values were averaged for each nutrient treatment (see Table 1, Figs. 1 and 2).

The "cornerpoints" are not presented in the DOM development plots, since both DIN and DIP in them were modified. Therefore, including these treatments could bias the interpretation of effects induced by single inorganic nutrients. However, in plots and analyses where DIP or DIN influence was investigated all treatments were included to avoid the single nutrient effect overestimation (see Figs. 3–5).

For an estimation of the drivers of changes in DOM optical properties, the covariance of total accumulation of DOM compounds (Δ_8DOM) with the cumulative sum of POM (Σ_{POM}) parameters was tested by linear regression analysis.

BGD
12, 7209–7255, 2015

Mean normalized deviations (mean dev. %), calculated as:

$$\text{mean dev } \% = \frac{100}{\overline{\Delta C} n} \sum_{\text{start}}^{\text{end}} \Delta C i(k) - \overline{\Delta C(k)}; \quad (5)$$

where C – is a concentration, absorption or fluorescence intensity, k – is the day of experiment, n – is a total number of days (n = end – start) and i – is a mesocosm ID (i = 1–16); $\Delta C i(k)$ is calculated by Eq. (4), $\overline{\Delta C(k)}$ – is the mean ΔC for all mesocosms at the day k, and $\overline{\Delta C}$ – is average ΔC for all mesocosms during the whole experiment. Mean dev. (%) were tested against nutrient supply (Varied P and Varied N) and DIN : DIP supply ratio in the mesocosms at day 2 in order to estimate the nutrient and stoichiometry effect on DOM accumulation in the mesocosms.

All statistical tests in this work were performed by the use of Sigma Plot 12.0 (Systat). The significance level accepted was $p < 0.05$.

3 Results

3.1 Particulate organic matter development

After nutrient addition, phytoplankton bloom development was observed in all mesocosms during both experiments. Maximum chl *a* concentrations in Varied P occurred at day 5 (Fig. 1a), with higher concentrations in treatments with initial nutrients supplied at lower or equal to Redfield N : P ratio (12.00N/0.75P, 12.00N/1.25P, 12.00N/1.75P). However, no significant relationship of the cumulative sums of chl *a* ($\Sigma_{\text{chl } a}$) to DIP concentration was recognized ($p > 0.05$, $n = 15$). In Varied N, chl *a* concentrations reached its maximum at day 6 (Fig. 1b) and $\Sigma_{\text{chl } a}$ were significantly affected by the initial DIN concentrations (Wilcoxon rank test: $p < 0.001$, $n = 16$), indicating that DIN was limiting phytoplankton biomass buildup.

Bacterial abundance increased until day 6 (paired t test: $p > 0.001$, $n = 31$) in all mesocosms and then stayed relatively constant towards the end of both experiments

BGD
12, 7209–7255, 2015

(paired t test: $p > 0.05$, $n = 31$; Fig. 1c and d). In Varied P, cumulative sums of bacterial abundance (Σ_{bac}) were not related to the initial DIP supply ($p > 0.05$, $n = 15$). Highest bacterial abundance was observed at day 6, yielding $2.0 \pm 0.7 \times 10^6$ mL^{-1} averaged for all treatments (Fig. 1c). In contrast, in Varied N, Σ_{bac} indicated significant covariance to DIN amendments ($p < 0.01$, $n = 16$). The highest bacterial abundance of $2.6 \pm 0.2 \times 10^6$ mL^{-1} was observed at day 6 in the treatment with the highest initial DIN concentration (20.00N/0.75P).

3.2 Dissolved organic matter

3.2.1 Dissolved organic matter abundance

Initial DOC concentrations (day 3), did not differ significantly between treatments in Varied P (one way ANOVA: $p > 0.05$, $n = 15$) and was 99 ± 5 µmol L^{-1} on average. In contrast, in Varied N initial DOC concentrations (day 2) varied significantly among mesocosms (Holm–Sidak test: $p < 0.001$, $n = 16$) with 87 ± 2 µmol L^{-1} in the treatment with second lowest initial DIN concentrations (4.00N/0.75P), 91 ± 1 µmol L^{-1} in the Redfield DIN : DIP treatment (12.00N/0.75P) and in the treatment with the lowest initial DIN concentrations (2.00N/0.75P), and 95 ± 3 µmol L^{-1} in the treatment with the highest initial DIN concentrations (20.00N/0.75P). The calculation of DOC accumulation (ΔDOC) thus allowed a better comparison of bulk DOC dynamics between treatments than absolute concentrations and will be given in following.

During both experiments, DOC accumulated significantly over time (paired t test: $p < 0.001$, $n = 31$) with higher accumulation observed in Varied N (Mann–Whitney rank sum test: $p < 0.001$, $n = 120$). On day 8, accumulation of DOC (Δ_8DOC) was highest (33 ± 23 µmol L^{-1}) in the highest DIP treatment (12.00N/1.75P) in Varied P (Fig. 2a), as well as in the highest DIN treatment (20.00N/0.75P) in Varied N (67 ± 3 µmol L^{-1}) (Fig. 2b).

Initial average CDOM absorption at 325 nm (a_{325}) was 0.17 ± 0.03 m^{-1} and 0.15 ± 0.01 m^{-1} for mesocosms of Varied P and Varied N, respectively (Fig. S1c, d in the

BGD
12, 7209–7255, 2015

Supplement). The starting CDOM absorption values were not significantly different between treatments (one way ANOVA: $p > 0.05$, $n = 31$). However, they differed between the two experiments (one way ANOVA: $p < 0.05$, $n = 31$). CDOM accumulation (Δa_{325}) will be given in following, as it allows a better comparison of CDOM dynamics between experiments than absolute absorption coefficients.

CDOM accumulated over time during both experiments (paired t test: $p < 0.001$, $n = 31$). CDOM accumulation on day 8 ($\Delta_8 a_{325}$) was the highest in the medium to high DIP treatment (12.00N/0.75P, 12.00N/1.25P, 12.00N/1.75P) in Varied P ($0.35 \pm 0.03\,m^{-1}$) (Fig. 2c) and in the highest DIN treatment (20.00N/0.75P) in Varied N ($0.48 \pm 0.13\,m^{-1}$) (Fig. 2d).

Spectral slopes, calculated within the 275–295 nm spectral range, ($S_{275–295}$) differed between treatments in the beginning of Varied N (one way ANOVA: $p < 0.05$, $n = 16$), whereas treatments in the beginning of Varied P were not significantly different (one way ANOVA: $p < 0.05$, $n = 15$). In contrast, initial values of spectral slopes, calculated within the 320–500 nm spectral range (S_{SEMO}), varied between treatments at the beginning of Varied P (one way ANOVA: $p < 0.05$, $n = 15$), but not at the beginning of Varied N (one way ANOVA: $p < 0.05$, $n = 16$). In order to avoid the influence of initial differences of spectral slopes on data analyses, daily changes in spectral slopes ($\Delta S_{275–295}$ and ΔS_{SEMO}) were calculated. More negative $\Delta S_{275–295}$ and ΔS_{SEMO} indicate that spectral slopes are decreasing. As spectral slope decrease, CDOM absorption at longer wavelengths becomes higher, indicating accumulation of HMW CDOM.

$S_{275–295}$ decreased over time in both experiments (paired t test: $p < 0.001$, $n = 31$). The most negative $\Delta S_{275–295}$ values ($-0.016 \pm 0.004\,nm^{-1}$ and $-0.014 \pm 0.002\,nm^{-1}$) were observed in the treatments with medium and high initial DIP concentrations (12.00N/0.75P, 12.00N/1.25P, 12.00N/1.75P) at the end (day 8) of Varied P (Fig. 2e) and in the treatment with the highest initial DIN concentrations (20.00N/0.75P) in at the end (day 8) of Varied N (Fig. 2f), respectively. Values for ΔS_{SEMO} decreased on average by $-7 \pm 3\,\mu m^{-1}$ from the beginning (day 3 and day 2) until the end (day 8) of both experiments (paired t test: $p < 0.001$, $n = 15, 16$). In general, ΔS_{SEMO} dynam-

BGD
12, 7209–7255, 2015

ics mirrored those of $\Delta S_{275-295}$. Both decreased faster in treatments with medium and high initial DIP concentrations (12.00N/0.75P, 12.00N/1.25P, 12.00N/1.75P) in Varied P and in treatment with the highest initial DIN concentrations (20.00N/0.75P) in Varied N (Table 2).

Derived from measured parameters, the ratio (S_R) of $S_{275-295}$ and spectral slopes, calculated within 350–400 nm wavelength range ($S_{350-400}$), had much larger uncertainties within treatments than spectral slopes themselves. The initial (day 3 and day 2) S_R were not statistically different among treatments in each experiment (one way ANOVA: $p > 0.05$, $n = 31$) and between experiments (one way ANOVA: $p > 0.05$, $n = 31$).

S_R increased only slightly over time in almost all mesocosms of Varied P (paired t test: $p < 0.05$, $n = 15$; Fig. 2g). In Varied N, S_R increased significantly on day 5 (paired t test: $p < 0.001$, $n = 16$) and decreased again slightly on day 7 (paired t test: $p < 0.05$, $n = 16$) in almost all mesocosms (Fig. 2h).

Three FDOM components with distinct spectral properties were identified during PARAFAC analysis of our dataset. The first FDOM component (Comp.1) was excited at 235 nm and emitted at 440–460 (300) nm, the second (Comp.2) and the third (Comp.3) FDOM components were excited at 275 (< 230) and 265 nm and emitted at 340 and 294 nm respectively (Table 3, Fig. S2).

The initial fluorescence of Comp.1 was 0.019 ± 0.001 Raman Units (RU) in Varied P and 0.0108 ± 0.0009 RU in Varied N. Initially, Comp.1 fluorescence was not significantly different between treatments in both, Varied P and Varied N (one way ANOVA: $p > 0.05$, $n = 31$) in contrast to initial differences between two experiments (one way ANOVA: $p < 0.01$, $n = 31$).

Subtracting the initial fluorescence of Comp.1 (ΔComp.1 calculating) allowed tracing the accumulation of freshly-produced Comp.1 during the experiments (Fig. 2i and j).

ΔComp.1 indicated an accumulation of Comp.1 over time in both experiments (paired t test: $p < 0.001$, $n = 31$). In Varied P, differences in ΔComp.1 fluorescence between treatments at the end of experiment were not significant (t test: $p > 0.05$, $n = 6$) and revealed 0.014 ± 0.004 RU on the average for all mesocosms (Fig. 2i). In Varied N,

BGD
12, 7209–7255, 2015

highest ΔComp.1 fluorescence intensities of 0.025 ± 0.004 RU were found in the treatment with highest DIN supply (20.00N/0.75P) (Fig. 2j). Here, clear differences were observed between treatments at the end of experiment (one way ANOVA: $p < 0.01$, $n = 11$).

The fluorescence intensities of Comp.2 were almost identical at the start of Varied P and Varied N, yielding 0.029 ± 0.005 RU and 0.029 ± 0.007 RU, respectively. No significant differences were observed between treatments (one way ANOVA: $p > 0.05$, $n = 31$) and experiments (one way ANOVA: $p > 0.05$, $n = 31$).

Comp.2 fluorescence increased in all mesocosms over time (paired t test: $p < 0.001$, $n = 31$) (Fig. 2k and l). At the end (day 8) of Varied P, the maximum ΔComp.2 fluorescence was 0.063 ± 0.007 RU in the treatment with highest DIP addition (12.00N/1.75P) (Fig. 2k). It was significantly higher than that in the treatment with the lowest initial DIP concentration (12.00N/0.25P) (t test: $p < 0.05$, $n = 6$) at day 8. Differences between treatments with the highest (20.00N/0.75P) and the lowest (2.00N/0.75P) initial DIN concentrations at the end (day 8) of Varied N were not significant (t test: $p > 0.05$, $n = 6$) and the maximum ΔComp.2 fluorescence comprised 0.04 ± 0.03 RU on average for all mesocosms (Fig. 2l).

The Comp.3 fluorescence intensity was highly variable during both experiments (Fig. 2m and n). Its starting values were not statistically different between Varied P and Varied N and comprised 0.03 ± 0.02 RU in both.

In Varied P, Comp.3 fluorescence intensity increased from start until day 5 (paired t test: $p < 0.05$, $n = 15$) and decreased after day 6 until end of experiment (paired t test: $p < 0.05$, $n = 15$) (Fig. 2m). In Varied N, Comp.3 accumulated significantly only after day 6 (paired t test: $p < 0.05$, $n = 16$) (Fig. 2n).

3.2.2 Assessing the origin of optically active dissolved organic matter

To investigate a potential influence of phytoplankton or bacteria abundances on DOC concentrations and CDOM and FDOM accumulation, cumulative sums of chl a ($\Sigma_{\text{chl } a}$)

BGD
12, 7209–7255, 2015

and bacterial abundance (Σ_{bac}) of each mesocosm (Sect. S3) were tested against total accumulation of DOM components at day 8 (Δ_8DOM) using linear regression analysis.

Values of Δ_8DOC correlated significantly with $\Sigma_{chl\ a}$ in Varied P ($p < 0.05$, $n = 15$) and in Varied N ($p < 0.001$, $n = 16$), but not with Σ_{bac} ($p > 0.05$, $n = 15$, 16, respectively).

To look at CDOM properties, the relationship between S_{SEMO} and a_{375} were compared to an Eq. (2) parametrization by Stedmon and Markager (2001) for marine CDOM of the Greenland Sea. In our study, no apparent differences between treatments were found and all data for S_{SEMO} vs. a_{375} could be expressed by Eq. (2). However, our data went beyond the limits defined by Stedmon and Markager, except those in the beginning of experiment (Fig. 3). Therefore, new parameterization of the Eq. (2) was obtained in this study by nonlinear least square fitting method (MATLAB, The MathWorks Inc.), with $\alpha = 17.5$ and $\delta = 0.2$.

Furthermore, CDOM accumulation ($\Delta_8 a_{325}$) correlated significantly to $\Sigma_{chl\ a}$ in Varied P ($p < 0.05$, $n = 15$) and Varied N ($p < 0.001$, $n = 16$), indicating that phytoplankton biomass was regulating CDOM dynamics in both experiments. While no covariance of $\Delta_8 a_{325}$ with Σ_{bac} was observed during Varied P ($p > 0.05$, $n = 15$), a significant correlation of $\Delta_8 a_{325}$ with Σ_{bac} ($r^2 = 0.33$, $p < 0.05$, $n = 16$) occurred in Varied N, indicating that bacteria may be partially responsible for CDOM dynamics under DIN stimulation.

ΔComp.1 behaved similar to Δa_{325} during both experiments. However, Δ_8Comp.1 was neither correlated to Σ_{bac} ($p > 0.05$, $n = 15$), nor to $\Sigma_{chl\ a}$ concentration ($p > 0.05$, $n = 15$) in Varied P. In contrast Δ_8Comp.1 was significantly correlated to both, $\Sigma_{chl\ a}$ ($p < 0.001$, $n = 16$) and Σ_{bac} ($p < 0.05$, $n = 16$) in Varied N.

Similar to Δ_8Comp.1, in Varied P, Δ_8Comp.2 did not reveal a significant relationship to $\Sigma_{chl\ a}$ ($p > 0.05$, $n = 15$) concentration or to Σ_{bac} ($p > 0.05$, $n = 15$). In Varied N, Δ_8Comp.2 also did not correlate to $\Sigma_{chl\ a}$ concentration ($p > 0.05$, $n = 16$), but it covariate significantly to Σ_{bac} ($p < 0.01$, $n = 16$), supporting a potential influence of bacterial abundance on fluorescence intensities of Comp.2.

BGD
12, 7209–7255, 2015

In contrast to Δ_8Comp.1 and Δ_8Comp.2, Δ_8Comp.3 did not covariate with Σ_{bac} ($p > 0.05$, $n = 15$, 16) nor with $\Sigma_{chl\ a}$ concentration ($p > 0.05$, $n = 15$, 16) in both experiments.

3.2.3 Effect of inorganic nutrients on optically active DOM

In order to access the nutrient influence on DOM accumulation, mean normalized deviations (mean dev. %) of ΔDOC, ΔCDOM (Δa_{325}) and ΔFDOM calculated for each mesocosm (including "corner" points) and tested against initial DIP supply in Varied P, and against initial DIN supply in Varied N using linear regression analysis (Fig. 4).

DOC accumulation was related to the initial inorganic nutrients supply in both experiments. Higher ΔDOC (mean dev. %) corresponded to higher DIP supply ($p < 0.05$, $n = 15$) in Varied P (Fig. 4a) and to higher DIN supply ($p < 0.05$, $n = 16$) in Varied N (Fig. 4b). However, no overall effect of DIN : DIP ratios was revealed when data from both experiments were combined ($p > 0.05$, $n = 31$). Therefore, accumulation of DOC, in general, was dependent rather on total initial amount of macronutrients, than on the relative concentration of DIN to DIP.

ΔCDOM (mean dev. %) correlated significantly to DIN supply ($p < 0.001$, $n = 14$) (Fig. 4c), but not to DIP supply ($p > 0.05$, $n = 15$) (Fig. 4d). Similar to ΔDOC (mean dev. %), no effect of initial DIN : DIP ratios on ΔCDOM (mean dev. %) were determined ($p > 0.05$, $n = 31$).

ΔComp.1 (mean dev. %) did not exhibit a significant relationship to the initial DIP supply ($p > 0.05$, $n = 15$) (Fig. 4e), but correlated significantly to the initial DIN concentrations ($p < 0.001$, $n = 12$) (Fig. 4f).

Oppositely, ΔComp.2 (mean dev. %) increased with initial DIP supply ($p < 0.05$, $n = 14$) (Fig. 4g), but not with initial DIN supply ($p > 0.05$, $n = 12$) (Fig. 4h). Thus, Comp.2 accumulation was higher under the higher DIP concentrations.

In contrast to both previous FDOM components, ΔComp.3 (mean dev. %) did not reveal covariance neither to DIP ($p > 0.05$, $n = 15$) (Fig. 4i), nor to DIN ($p > 0.05$, $n = 12$) initial supply (Fig. 4n).

BGD
12, 7209–7255, 2015

No overall effect of DIN : DIP ratios on ΔComp.1, ΔComp.2 and ΔComp.3 (mean dev. %) was determined when data from both experiments were combined ($p > 0.05$, $n = 27$).

Hence, accumulation of Comp.1 was dependent on the initial DIN concentrations, accumulation of Comp.2 increased with increase of initial DIP concentrations and Comp.3 was unaffected by nutrient treatments.

3.2.4 Nutrients effects on the relationship between CDOM and DOC

To investigate the relationship between CDOM absorption and DOC concentrations during the course of the experiments, daily DOM accumulation (ΔDOC) was tested against daily accumulation of CDOM at 325 nm (Δa_{325}) by linear regression analysis for each mesocosm and for all data combined (Fig. 5a and b). Direct relationships were observed between ΔDOC and Δa_{325} in both, Varied P ($p < 0.001$, $n = 75$) and Varied N ($p < 0.001$, $n = 95$).

The estimated slopes of those linear regressions, for each mesocosm for Δa_{325} vs. ΔDOC, were tested for correlation with the initial DIP (Fig. 5c) and DIN (Fig. 5d) concentrations. Estimated slope values significantly increased with initial DIN supply ($p < 0.01$, $n = 16$), indicating that the CDOM fraction of DOC was affected by nutrient availability and specifically by DIN supply.

Although the relationship between CDOM and DOC revealed a dependency on initial DIN supply, the values of CDOM at 355 nm (a_{355}) to DOC ratio (a_{355}/DOC) did not reveal a significant nutrient effect, when plotted against $S_{275–295}$ (Fig. 5e).

All data of $S_{275–295}$ and a_{355}/DOC of our study can be described by the Eq. (3) with coefficients, derived by Fichot and Benner (2012) for calculations of DOC concentrations. All our data points were fitting to 8 % uncertainty interval of estimation of DOC concentrations, defined by Fichot and Benner (2012) (Fig. 5e).

BGD
12, 7209–7255, 2015

4 Discussion

Optically active DOM and its properties are often used for estimation of DOC concentrations and processes, influencing DOM. CDOM was previously shown to accumulate along with the remineralization of inorganic nutrients (Zhang et al., 2009) and therefore, was assumed as an indicator of bacterial DOM reworking (Swan et al., 2009; Nelson and Siegel, 2013). However, CDOM was also shown to be consumed during dark incubations (Zhang et al., 2009), and therefore characterized as containing fresh and labile DOM. For discrimination between freshly released by phytoplankton and microbially altered CDOM pools, specific properties of the CDOM spectrum are commonly used. Spectral slopes, for instance, can indicate a relative changes in HMW-CDOM proportion in CDOM (Helms et al., 2008). Spectral slope ratios were used before to discriminate between biogeochemical processes influencing CDOM (Helms et al., 2008). Fluorescent fraction of CDOM (FDOM) is used for better characterization and discrimination between DOM pools with different spectral and therefore structural properties (Coble, 1996; Gueguen and Kowalczuk, 2013). Here, we investigated nutrient effects on the production, accumulation and cycling of CDOM and FDOM, as well as nutrient effects on relationship between CDOM absorption and DOC concentrations.

4.1 Nutrient effects on the production and cycling of optically active DOM

Our results indicated that chl *a* accumulation and bacterial growth were stimulated by DIN supply. Along with the response of POM production to inorganic nutrient amendments, changes in the optically active DOM fractions were observed.

Initial DOC concentrations, measured in both experiments (Fig. S1a, b), were in the range or slightly higher of those previously reported and modelled for the upper 30 m of the ETNA watercolumn (Hansell et al., 2009).

In both experiments, DOC accumulated over time (Fig. 2a and b) and seemed to be produced mainly by phytoplankton release. The highest DOC accumulation was observed on the moment of rapid transition from nutrient replete to nutrient depleted

BGD
12, 7209–7255, 2015

conditions (see Engel et al., 2015). That is in line with previous studies (Engel et al., 2002; Conan et al., 2007; Carlson and Hansell, 2015) showing DOM accumulation after the onset of nutrient limitation, while the chl *a* signal decreased.

An effect of initial nutrient concentration on DOC accumulation (Fig. 4a and b), observed in our study, was shown previously. In a mesocosm study with ETNA waters, Franz et al. (2012) observed that higher DOC concentrations developed when the initial inorganic nitrogen supply was high. As well, DOC concentrations in their study were even higher when high DIN concentrations were combined with high DIP supply. In their mesocosm experiment in Arctic, Conan et al. (2007) and Stedmon and Markager (2005) observed that at silicate-replete conditions, DOC concentrations under high initial DIN supply did not vary significantly from those under high initial DIP concentrations. In our study, silicate was also not limiting phytoplankton growth and higher DOC concentrations occurred at higher DIP as well as at higher DIN concentrations, supporting earlier findings.

Bacterial turnover may have influenced the composition of DOM (as it is seen by changes in spectral slope ratios and FDOM components) while DOC concentrations seemed to be not related to bacterial abundances. This observation may be explained by rapid bacterial consumption of labile DOM accompanied by the bacterial release of altered humic-like DOM (Azam et al., 1983; Ogawa et al., 2001), which are therefore not influencing measured DOC concentrations (e.g. Kirchman, 1991).

CDOM absorptions were in the range of those previously reported for open waters of the Atlantic Ocean at the beginning of the experiment, while the final CDOM absorptions were twice as high (Fig. S1c, d; Nelson et al., 2009; Nelson and Siegel, 2012; Swan et al., 2013). Similar to our experiments, CDOM absorption was previously shown to accumulate by factor of 2 to 3 during mesocosm studies (Zhang et al., 2009; Pavlov et al., 2014).

In our experiments, the accumulation of CDOM during the phytoplankton bloom (Fig. 2c and d) as well as significant covariance to phytoplankton pigment (chl *a*) suggests that phytoplankton was the major source of CDOM. This is consistent with

BGD
12, 7209–7255, 2015

previous studies that show CDOM to be produced by extracellular release from phytoplankton (Romera-Castillo et al., 2010) or by phytoplankton degradation or lysis (Hu et al., 2006; Zhang et al., 2009; Organelli et al., 2014).

Changes in CDOM spectral properties, such as the decrease of CDOM spectral slopes over time (Fig. 2e and f), indicated that absorption in the visible wavelength range increased relatively to the UV wavelength range. As the absorption at longer wavelength is corresponding to larger molecules, we may assume that HMW-CDOM accumulated during both experiments. HMW-DOM was previously shown to be more labile for bacterial consumption than low molecular weight DOM (at molecular weight cutoff of 1 kDa) (Benner and Amon, 2015), as bacterial activity was higher, when incubating with HMW-DOM (Amon and Benner, 1996). Furthermore HMW-DOM is typically accounting to 30 to 60 % of the total DOM released via phytoplankton (Biddanda and Benner, 1997; Engel et al., 2011). Therefore we consider the spectral slope decrease over time as an indication of labile CDOM production via phytoplankton release.

In treatments with high initial DIN concentrations, bacterial abundance was significantly higher than in those at lower initial DIN concentrations. Furthermore, bacterial abundances correlated significantly to CDOM concentrations. We therefore suggest that higher bacterial abundance may have been responsible for an additional production of CDOM in mesocosms, particularly in those, where initial DIN supply was high.

This suggestion is made also based on changes in optical properties during our study. As Zhang et al. (2009) showed before, the spectral slope ratio (S_R) decreases, when bacterial modification of CDOM takes place. A slight decrease of S_R towards the end of Varied N (Fig. 2h), most likely indicated that CDOM was reworked by bacteria. The idea of an additional CDOM production by bacteria in this experiment is also in agreement with previous studies, where DOM bacterial reworking was indicated as CDOM source (Rochelle-Newall and Fisher, 2002; Nelson et al., 2004; Nelson and Siegel, 2013; Swan et al., 2009).

However, due to its large uncertainties within treatments, S_R was not sufficient to estimate the degree of bacterial CDOM production, most likely due to screening of the ef-

BGD
12, 7209–7255, 2015

fect by simultaneous high HMW-DOM production via phytoplankton release. Therefore, CDOM production via phytoplankton release, which occurred proportionally to phytoplankton biomass, was likely more pronounced than CDOM production via bacterial reworking of labile DOM.

The CDOM to DOC ratio was also affected by variable initial DIN concentrations. A significant positive correlation of CDOM accumulation over time with DOC concentration was found in both experiments (Fig. 5a and b), indicating that DOC and CDOM had been affected by the same processes. Estimated slopes of ΔCDOM against ΔDOC (Fig. 5d) were highest at highest initial DIN concentrations in Varied N, indicating that relative proportion of CDOM in bulk DOM may be regulated by presence of DIN.

Factors, influencing the ratio between CDOM absorption and DOC concentrations are little understood so far. It is known that CDOM absorption often co-varies with DOC concentration in river estuaries and coastal seas, which are influenced to a high degree by conservative mixing of riverine and marine waters (Nelson and Siegel, 2013; Rochelle-Newall et al., 2014). However, in the open ocean, the relation is losing its consistency (Nelson and Siegel, 2013).

We suggest that, under higher initial DIN concentrations, higher bacterial abundance and hence higher bacterial reworking of DOM, the proportion of the colored fraction in DOM increases. Our results suggest that an increase of initial DIN concentrations by $10\,\mu mol\,L^{-1}$ would increase CDOM accumulation (Δa_{325}) relative to DOC concentrations (ΔDOC) by $1.4 \times 10^{-3}\,m^{-1}\,\mu mol^{-1}\,L$ (see Fig. 5d). The change however is small, compared to those, caused by other factors, as, for instance, mixing and photochemical oxidation (Stedmon and Nelson, 2015). However, the effect may be important in regimes or at times of large changes in DIN concentrations.

When CDOM properties, such as spectral slopes $S_{275–295}$, were also taken into account, the variance of relationship between CDOM (a_{355}) and DOC between treatments was not apparent (Fig. 5e). We found a good correspondence between $S_{275–295}$ and a_{355}/DOC ratio during our study, which could be explained by the model of Fichot and Benner (2012).

BGD
12, 7209–7255, 2015

Although the model was developed for DOC calculation from CDOM absorption and the spectral slope in river estuaries, our data fitted to the model limits. Therefore our data support the findings of Fichot and Benner (2012) of a stable $S_{275–295}$ to a_{355}/DOC relationship.

The model assumption is that changes in relative molecular weight and CDOM absorption are proportional to changes in DOC concentrations. This relation, therefore, may be useful for field studies, where optical measurements are available only. For remote sensing, however, an application of this relationship would be rather difficult, since ocean color remote sensing measurements are limited to an "optical window" of visible to near-infrared wavelength range (IDRISI Guide to GIS and Image Processing, 2006).

More sensitive to nutrient amendments were FDOM fractions, of which three different fluorescent components could be identified during this study (Fig. S2).

The characteristics of the first component, Comp.1 (Table 3), were similar to those of the humic-like peak "A" described by Coble et al. (1996). The Comp.1 fluorescence was within the reported range of A-like peak fluorescence intensities for the open ocean area (Jorgensen et al., 2011) or slightly higher towards the end of experiments depending on mesocosm treatment.

Previous studies of Stedmon and Markager (2005), Kowalczuk et al. (2009) and Zhang et al. (2009) showed that humic-like components, similar by spectral properties to Comp.1, are produced via microbial DOM reworking (Table 3, Fig. S1i, j).

In our study, in Varied N, Comp.1 was strongly correlated to initial DIN concentrations, as the final Comp.1 fluorescence intensity was almost three fold higher at the highest initial DIN supply than that in the treatments with lowest DIN supply. Thus, since bacterial abundance was DIN dependent in this experiment and Comp.1 fluorescence intensities correlated significantly to bacterial abundances, the bacteria were likely responsible for Comp.1 occurrence during our experiments. In Varied P, Comp.1 was not related to bacterial abundance. Similar initial DIN concentrations in all mesocosms may be a reason of the absence of covariance of Comp.1 with bacteria, since no

BGD
12, 7209–7255, 2015

significant differences between treatments were noticed for bacterial abundance and also only a little difference was noticed for Comp.1. Therefore, bacterial abundance may still be responsible for Comp.1 accumulation in this experiment. Also, if Comp.1 is bacterially mediated, its higher abundances in the end of our experiments compared to those in the open ocean may be explained by higher substrate availability in the mesocosms than that in the North Atlantic.

The fluorescence properties of the second FDOM component, Comp.2 (Table 3, Fig. S2), were similar to that of the previously defined amino acid-like fluorescence (Mopper and Schulz, 1993; Coble et al., 1996; Stedmon and Markager, 2005): tryptophan-like peak 'T' (Coble et al., 1996). The fluorescence intensities of this component were in the range of that previously reported for open ocean area (Jorgensen et al., 2011) for the whole experimental period (Fig. S1k, l).

Similar by spectral properties to Comp.2, amino acid-like compounds were previously hypothesized to represent the fluorescence of the bound-to-protein matrix amino acids tryptophan and tyrosine (Stedmon and Markager, 2005) and were assumed to be produced by phytoplankton (Mopper and Schulz, 1993; Coble et al., 1996). We therefore consider Comp.2 as indicator of phytoplankton-produced proteinaceous DOM and as possible precursor for humic-like FDOM.

In Varied P, Comp.2 accumulated proportionally to initial DIP concentrations and its abundances were not corresponding to chl *a* concentrations. This might indicate that proteinaceous DOM release by phytoplankton is controlled by nutrient availability, rather than by phytoplankton biomass itself, i.e. proteinaceous DOM is produced as a part of an overflow mechanism (Carlson and Hansell, 2015) of extracellular release.

In Varied N, again no covariance of Comp.2 to chl *a* was determined. However, a covariance of Comp.2 with initial DIN concentrations did not occur as well. As bacteria were more abundant in treatments with higher initial DIN supply and also Comp.2 intensities revealed significant correspondence to bacteria, we suggest that bacteria abundance may have regulated Comp.2 fluorescence intensities, particularly under high initial DIN concentrations.

BGD
12, 7209–7255, 2015

Previously, Stedmon and Markager (2005) showed an accumulation of a FDOM component, with spectral properties similar to Comp.2, during their mesocosm study treatments of high DIN and high DIP concentrations. This component was also shown to be consumed during dark and light incubations, when bacteria were added. Kirchman et al. (1991) showed that DOM uptake can be accompanied by a decrease in DIN concentrations, indicating the importance of DIN presence during bacterial reworking of labile DOM.

Therefore, Comp.2 production might be dependent on initial DIP and DIN availability, similarly to the increase of DOC concentrations. As well as at high initial DIN concentrations, Comp.2 may be reworked by bacteria to humic-like Comp.1.

The spectral properties of the third fluorescent component (Comp.3) were similar to that of amino acid-like fluorescence (Table 3) (Mopper and Schulz, 1993; Coble et al., 1996; Stedmon and Markager, 2005): tyrosine-like peak "B" (Coble et al., 1996) and were in the range of those previously reported for open ocean area (Jorgensen et al., 2011).

The development patterns as well as no clear response towards nutrient amendments of Comp.3 made it very difficult for interpretation.

Comp.3 fluorescence intensities increased at the day of chl *a* maximum in Varied P (Fig. 2m), suggesting that Comp.3 could be released by phytoplankton during its growth. Rapid bacterial reworking of amino acid-like material may have occurred as well in this experiment and therefore, Comp.3 may have been consumed by bacteria after the chl *a* maximum. However, it could also be modified to Comp.2 in Varied P.

In Varied N, Comp.3 fluorescence intensities were significantly higher only at the end of experiment (Fig. 2n). Comp.3 accumulation at the end of this experiment could indicate bacterial reworking of the higher in molecular weight Comp.2 with release of Comp.3 as byproduct. On the other hand, Comp.3 accumulation towards the end of this experiment could be a result of higher amounts of amino acids within degrading phytoplankton tissues, which were still released, after chl *a* concentration had decreased.

BGD
12, 7209–7255, 2015

A fluorescent substance, similar by spectral properties to Comp.3, was previously hypothesized to represent the tryptophan and tyrosine in peptides (Stedmon and Markager, 2005), and it was also previously found accumulating during the denaturation of proteins (Determann et al., 1998). No effect of microbial degradation was found on the abundance of this fluorescence substance in dark and light incubations with bacteria (Stedmon and Markager, 2005). However, as this substance was removed during mesocosm experiment, spontaneous abiotic aggregation or photochemically induced flocculation were hypothesized as possible removal mechanisms.

For our study, we therefore assume that, Comp.3 potentially acted as an intermediate product during formation or degradation of proteinaceous Comp.2. Still, the interpretation of the Comp.3 development remains speculative.

It was hypothesized previously that phosphorus limitation leads to accumulation of DOM more resistant to microbial degradation (Kragh and Sondergaard, 2009), e.g. due to phytoplankton extracellular release of this "poor quality" DOM or limitation of bacterial DOM consumption (Carlson and Hansell, 2015). Based on changes in optical DOM properties (S_R, Comp.1, Comp.2) in our study, we suggest that labile DOM in the ETNA accumulates proportionally to either high DIN or high DIP concentrations. However, the "poor quality" DOM accumulates more under high DIN concentrations (i.e. phosphorus limitation), due to bacterial DOM reworking. And even though bacterial activity per cell might have been limited by phosphorus availability, higher bacterial abundance in treatments with higher initial DIN supply would lead to more pronounced net accumulation of more resistant to microbial degradation DOM.

Overall, during both of our experiments, the variance of CDOM absorption values and FDOM components within the treatment with Redfield ratio of DIN : DIP of 16 (12.00N/0.75P) of each experiment was higher than variance between experiments. Therefore, the nutrient effects for CDOM and FDOM components were considered much stronger, than effects, caused by other factors. However, the difference in development pattern for some optically active parameters (S_R, Comp.3) suggests that influence by additional factors may have influenced results and cannot be excluded.

BGD
12, 7209–7255, 2015

4.2 Can marine CDOM in Tropical Ocean be predicted?

When comparing our data to the empirical model, developed by Stedmon and Markager (2001) for discrimination between marine and riverine CDOM, the data from our mesocosms experiments did not fit to the model limits.

This model was developed for Arctic seas and was used successfully for separation of terrestrially originated CDOM from marine CDOM in the Arctic during mesocosm (Pavlov et al., 2014) and field studies (Granskog et al., 2012).

The model represents a parametrized Eq. (2), where $\alpha = 7.4$ and $\beta = 1.1$ with model limits, defined by authors as 4 SD, which was calculated from results of dilution series (see Stedmon and Markager, 2001). Thus, all data, which lie on the model curve and do not exceed the model limits (Fig. 3), are considered as in situ-produced marine CDOM. Those CDOM absorptions vs. spectral slope values, which do not fit to model limits, are considered as allochthonous or riverine CDOM.

Although our data did not fit the model limits, other origin than in situ production is hard to imagine for CDOM produced during our mesocosm study. Other factors, such as strong differences in environmental conditions, e.g. temperature, salinity, light availability, DOM background concentrations, DOM availability, as well as differences in microbial communities of Arctic compared to ETNA waters, can be responsible for this inconsistency.

The difference between our data and the Stedmon and Markager (2001) model prediction is caused mainly by higher spectral slope values (S_{SEMO}) of CDOM spectra. Insolation differences, between the region where the model was developed and the ETNA may be responsible for changes of CDOM spectral slope properties, as CDOM enters photoreactions (Sulzberger and Durisch-Kaiser, 2008). Those photoreactions are primarily affecting the absorption in the visible wavelength range of light spectra producing uncolored and biologically available or refractory DOM (Benner and Amon, 2015). This could result in the reduction of CDOM absorption at higher wavelength and therefore explain an increase of spectral slope values.

BGD
12, 7209–7255, 2015

We therefore suggest that care needs to be taken when using empirically derived models from different regions. Based on data from our mesocosm experiments, we give a new parametrization for surface waters of ETNA, that is:

$$S_{\mathrm{SEMO}} = 17.5 + 0.2/a_{375}.$$

However, because this parametrization is based solely on our mesocosm experiments, affected by high nutrient input and phytoplankton bloom conditions, as well as absence of mixing, it needs to be reexamined in field studies in Tropical Ocean.

5 Conclusions

Our study shows that during phytoplankton blooms DOM is largely derived from phytoplankton, while its optical properties undergo considerable changes due to bacterial reworking. Thus, optically active proteinaceous substances are freshly produced by phytoplankton release. They are, however, consumed and reworked by bacteria, leading to accumulation of less-bioavailable optically active humic substances.

Our experiments indicate that DIN is the major macronutrient regulating the accumulation of bacterially originated optically active humic substances, while the accumulation of labile proteinaceous substances via phytoplankton is rather regulated by DIN and DIP. An input of humic substances can increase CDOM/DOC ratio and therewith affect predictions of DOC concentration based on CDOM absorbance.

Furthermore, our study contributes to the validation of the model developed by Fichot and Benner (2012). Our data suggest that this model could be used for an estimation of DOC concentrations in open waters of ETNA.

The Supplement related to this article is available online at doi:10.5194/bgd-12-7209-2015-supplement.

BGD
12, 7209–7255, 2015

Acknowledgements. This study was sponsored SFB754 project, "Climate–Biogeochemical Interactions in the Tropical Ocean" DFG. We thank all participants of Cabo Verde 2012 research stay for joint work during water sampling and handling of mesocosms and N. Vieira for help with initial water sampling. We also thank I. Monteiro, M. Schütt and P. Silva for help with logistics.

We are very grateful to P. Kowalczuk for valuable comments during our PARAFAC analysis, J. Roa for DOC analyses, U. Pankin for nutrient measurements, and S. Endres, L. Galgani, R. Flerus and C. Löscher for helpful discussions during the manuscript writing.

All data will be available at www.pangaea.de upon publication of the manuscript.

The article processing charges for this open-access publication were covered by a Research Centre of the Helmholtz Association.

References

Amon, R. M. W. and Benner, R. Bacterial utilization of different size classes of dissolved organic matter, Limnol. Oceanogr., 41, 41–51, 1996.

Azam, F., Fenchel, T., Field, J. G., Gray, J. S., Meyer-Reil, L. A., and Thingstad, F.: The ecological role of water-column microbes in the sea, Mar. Ecol.-Prog. Ser., 10, 257–263, 1983.

Benner, R. and Amon, R. M. W.: The size-reaktivity continuum of major bioelements in the ocean, Annu. Rev. Mar. Sci., 7, 2.1–2.21, 2015.

Biddanda, B. and Benner, R.: Carbon, nitrogen and carbohydrate fluxes during the production of particulate and dissolved organic matter by marine phytoplankton, Limnol. Oceanogr., 42, 506–518, 1997.

Brandt, P., Bange, H. W., Banyte, D., Dengler, M., Didwischus, S.-H., Fischer, T., Greatbatch, R. J., Hahn, J., Kanzow, T., Karstensen, J., Körtzinger, A., Krahmann, G., Schmidtko, S., Stramma, L., Tanhua, T., and Visbeck, M.: On the role of circulation and mixing in the ventilation of oxygen minimum zones with a focus on the eastern tropical North Atlantic, Biogeosciences, 12, 489–512, doi:10.5194/bg-12-489-2015, 2015.

Bricaud, A., Morel, A., and Prieur, L.: Absorption by dissolved organic matter of the sea (yellow substance) in the UV and visible domain, Limnol. Oceanogr., 26, 43–53, 1981.

BGD

12, 7209–7255, 2015

Carlson, C. A. and Hansell, D. A. (Eds.): DOM Sources, Sinks, Reactivity and Budgets, in: Biogeochemistry of Marine Dissolved Organic Matter, 2nd edn., Elsevier, Eastbourne, UK, 66–126, 2015

Coble, P. G.: Characterisation of marine and terrestrial DOM in seawater using excitation-emission matrix spectroscopy, Mar. Chem., 51, 325–346, 1996.

Coble, P. G.: Marine optical biogeochemistry: the chemistry of ocean color, Chem. Rev., 107, 402–418, doi:10.1021/cr050350+, 2007.

Conan, P., Søndergaard, M., Kragh, T., Thingstad, F., Pujo-Pay, M., le B. Williams, P. J., Markager, S., Cauwet, G., Borch, N. H., Evans, D., and Riemann, B.: Partitioning of organic production in marine plankton communities: the effects of inorganic nutrient ratios and community composition on new dissolved organic matter, Limnol. Oceanogr., 52, 753–765, 2007.

De Haan, H. and De Boer, T.: Applicability of light absorbance and fluorescence as measures of concentration and molecular size of dissolved organic carbon in humic Laken Tjeukemeer, Water Res., 21, 731–734, 1987.

Del Castillo, C. E.: Remote sensing of organic matter in coastal waters, in: "Remote Sensing of Coastal Aquatic Environments: Technologies, Techniques and Applications", edited by: Miller, R. L., Del Castillo, C. E., and McKnee, B. A., Springer, Dordrecht, The Netherlands, 157–180, 2005.

Del Vecchio, R. and Blough, N. V.: On the origin of the optical properties of humic substances, Environ. Sci. Technol., 38, 3885–3891, 2004.

Determann, S., Lobbes, J. M., Reuter, R., and Rullköter, J.: Ultraviolet fluorescence excitation and emission spectroscopy of marine algae and bacteria, Mar. Chem., 62, 137–156, 1998.

Engel, A., Goldthwait, S., Passow, U., and Alldredge, A.: Temporal decoupling of carbon and nitrogen dynamics in a mesocosm diatom bloom, Limnol. Oceanogr., 47, 753–761, 2002.

Engel, A., Händel, N., Wohlers, J., Lunau, M., Grossart, H.-P., Sommer, U., and Riebesell, U.: Effects of sea surface warming on the production and consumption of dissolved organic matter during phytoplankton blooms: results from a mesocosm study, J. Plankton Res., 33, 357–372, 2011.

Engel, A., Borchard, C., Loginova, A., Meyer, J., Hauss, H., and Kiko, R.: Effects of varied nitrate and phosphate supply on polysaccharidic and proteinaceous gel particles production during tropical phytoplankton bloom experiments, Biogeosciences Discuss., 12, 6589–6635, doi:10.5194/bgd-12-6589-2015, 2015.

BGD
12, 7209–7255, 2015

Fanning, K. A.: Nutrient provinces in the sea: concentration ratios, and ideal covariation, J. Geophys. Res., 97, 5693–5712, 1992.
Fichot, C. G. and Benner, R.: A novel method to estimate DOC concentrations from CDOM absorption coefficients in coastal waters, Geophys. Res. Lett., 38, L03610, doi:10.1029/2010GL046152, 2011.
Fichot, C. G. and Benner, R.: The spectral slope coefficient of chromophoric dissolved organic matter ($S_{275–295}$) as a tracer of terrigenous dissolved organic carbon in river-influenced ocean margins, Limnol. Oceanogr., 57, 1453–1466, doi:10.4319/lo.2012.57.5.1453, 2012.
Franz, J. M. S., Hauss, H., Sommer, U., Dittmar, T., and Riebesell, U.: Production, partitioning and stoichiometry of organic matter under variable nutrient supply during mesocosm experiments in the tropical Pacific and Atlantic Ocean, Biogeosciences, 9, 4629–4643, doi:10.5194/bg-9-4629-2012, 2012.
Granskog, M. A., Macdonald, R. W., Mundy, C. J., and Barber, D. G.: Distribution, characteristics and potential impacts of chromophoric dissolved organic matter (CDOM) in Hudson Strait and Hudson Bay, Canada, Cont. Shelf Res., 27, 2032–2050, 2007.
Gruber, N. and Sarmento, J. L.: Global patterns of marine nitrogen fixation and denitrification, Global Biogeochem. Cy., 11, 235–266, 1997.
Guéguen, C. and Kowalczuk, P.: Colored dissolved organic matter in frontal zones, in: Chemical Oceanography of Frontal Zones, edited by: Belkin, I., Springer-Verlag, Berlin, in press, pp. 35, doi:10.1007/698_2013_244, 2013.
Hansell, D. A.: Dissolved organic carbon reference material program, EOS, 86, 318, 2005.
Hansell, D. A., Carlson, C. A., Repeta, D. J., and Shitzer, R.: Dissolved organic matter in the ocean: a controversy stimulated new insights, Oceanography, 22, 202–211, 2009.
Hauss, H., Franz, J. M. S., Hansen, T., Struck, U., and Sommer, U.: Relative inputs of upwelled and atmospheric nitrogen to the eastern tropical North Atlantic food web: spatial distribution of δ^{15}N in meso zooplankton and relation to dissolved nutrient dynamics, Deep-Sea Res. Pt. I, 75, 135–145, doi:10.1016/j.dsr.2013.01.010, 2013.
Helms, J. R., Stubbins, A., Ritchie, J. D., and Minor, E. C.: Absorption spectral slopes and slope ratios as indicators of molecular weight, source, and photobleaching of chromophoric dissolved organic matter, Limnol. Oceanogr., 53, 955–969, 2008.
Hu, C., Lee, Z., Muller-Karger, F. E., Carder, K. L., and Walsh, J. J.: Ocean color reveals phase shift between marine plants and yellow substance, IEEE Geosci. Remote S., 3, 262–266, 2006.

BGD
12, 7209–7255, 2015

IDRISI Guide to GIS and Image Processing: Volume 1, available at: https://www.mtholyoke.edu/courses/tmillett/course/geog205/files/remote_sensing.pdf (last access: 23 April 2015), 2006.

Ishii, S. K. L. and Boyer, T. H.: Behavior of reoccurring PARAFAC components in fluorescent dissolved organic matter in natural and engineered systems: a critical review, Environ. Sci. Technol., 46, 2006–2017, doi:10.1021/es2043504, 2012.

Jayakumar, A., O'Mullan, G. D., Naqvi, S. W. A., and Ward, B. B.: Denitrifying bacterial community composition changes associated with stages of denitrification in oxygen minimum zones, Microb. Ecol., 58, 350–362, doi:10.1007/s00248-009-9487-y, 2009.

Jetten, M. S., Niftrik, L., Strous, M., Kartal, B., Keltjens, J. T., and Op den Camp, H. J.: Biochemistry and molecular biology of anammox bacteria, Crit. Rev. Biochem. Mol., 44, 65–84, doi:10.1080/10409230902722783, 2009.

Jiao, N., Herndl, G. J., Hansell, D. A., Benner, R., Kattner, G., Wilhelm, S. W., Kirchman, D. L., Weinbauer, M. G., Luo, T., Chen, F., and Azam, F.: Microbial production of recalcitrant dissolved organic matter: long-term carbon storage in the global ocean, Nat. Rev. Microbiol., 8, 593–599, doi:10.1038/nrmicro2386, 2010.

Jørgensen, L., Stedmon, C. A., Kragh, T., Markager, S., Middelboe, M., and Søndergaard, M.: Global trends in the fluorescence characteristics and distribution of marine dissolved organic matter, Mar. Chem., 126, 139–148, doi:10.1016/j.marchem.2011.05.002, 2011.

Karstensen, J., Stramma, L., and Visbeck, M.: Oxygen minimum zones in the eastern tropical Atlantic and Pacific oceans, Prog. Oceanogr., 77, 331–350, doi:10.1016/j.pocean.2007.05.009, 2008.

Karstensen, J., Fiedler, B., Schütte, F., Brandt, P., Körtzinger, A., Fischer, G., Zantopp, R., Hahn, J., Visbeck, M., and Wallace, D.: Open ocean dead zones in the tropical North Atlantic Ocean, Biogeosciences, 12, 2597–2605, doi:10.5194/bg-12-2597-2015, 2015.

Kartal, B., Kuypers, M. M., Lavik, G., Schalk, J., Op den Camp, H. J., Jetten, M. S., and Strous, M.: Anammox bacteria disguised as denitrifiers: nitrate reduction to dinitrogen gas via nitrite and ammonium, Environ. Microbiol., 9, 635–642, 2007.

Kieber, R. J., Zhou, X., and Mopper, K.: Formation of carbonyl compounds from UV-induced photodegradation of humic substances in natural waters: fate of riverine carbon in the sea, Limnol. Oceanogr., 35, 1503–1515, 1990.

Kieber, R. J., Li, A., and Seaton, P. J.: Production of nitrite from photodegradation of dissolved organic matter in natural waters, Environ. Sci. Technol., 33, 993–998, 1999.

BGD
12, 7209–7255, 2015

Kirchman, D. L., Suzuki, Y., Garside, C., and Duklow, H. W.: High turover rates of dissolved organic carbon during a spring phytoplankton bloom, Letters to Nature, 325, 612–614, 1991.
Kowalczuk, P., Durako, M. J., Young, H., Kahn, A. E., Cooper, W. J., and Gonsior, M.: Characterisation of dissolved organic matter fluorescence in the South Atlantic Bight with the use of PARAFAC model: interannual variability, Mar. Chem., 113, 182–196, 2009.
Kragh, T. and Sondergaard, M.: Production and decomposition of new DOC by marine plankton communities: carbohydrates, refractory components and nutrient limitation, Biogeochemistry, 96, 177–187, 2009.
Mathis, J. T., Pickart, R. S., Hansell, D. A., Kadko, D., and Bates, N. R.: Eddy transport of organic carbon and nutrients from the Chukchi Shelf: impact on the upper halocline of the western Arctic Ocean, J. Geophys. Res., 112, C05011, doi:10.1029/2006JC003899, 2007.
McGillicuddy Jr., D. J., Anderson, L. A., Doney, S. C., and Maltrud, M. E.: Eddy-driven sources and sinks of nutrients in the upper ocean: result from a 0.1° resolution model of the north Atlantic, Global Biogeochem. Cy., 17, 1035, doi:10.1029/2002GB001987, 2003.
McGillicuddy Jr., D. J., Anderson, L. A., Bates, N. R., Bibby, T., Buesseler, K. O., Carlson, C. A., Davis, C. S., Ewart, C., Falkowski, P. G., Goldthwait, S. A., Hansell, D. A., Jenkins, W. J., Johnson, R., Kosnyrev, V. K., Ledwell, J. R., Li, Q. P., Siegel, D. A., and Steinberg, D. K.: Eddy/wind interactions stimulate extraordinary mid-ocean plankton blooms, Science, 316, 1021–1026, doi:10.1126/science.1136256, 2007.
Mopper, K. and Schultz, C. A.: Fluorescence as possible tool for studying the nature of water column distribution of DOC components, Mar. Chem., 41, 229–238, 1993.
Mopper, K., Stubbins, A., Ritchie, J. D., Bialk, H. M., and Hatcher, P. G.: Advanced instrumental approaches for characterization of marine dissolved organic matter: extraction techniques, mass spectrometry, and nuclear magnetic resonance spectroscopy, Chem. Rev., 107, 419–442, doi:10.1021/cr050359b, 2007.
Moran, M. A. and Zepp, R. G.: Role of photoreactions in the formation of biologically labile compounds from dissolved organic matter, Limnol. Oceanogr., 42, 1307–1316, 1997.
Murphy, K. R., Stedmon, C. A., Graeber, D., and Bro, R.: Fluorescence spectroscopy and multy-way techniques, PARAFAC, Anal. Methods, 5, 6557–6566, doi:10.1039/c3ay41160e, 2013.
Nelson, N. B. and Siegel, D. A.: The global distribution and dynamics of chromophoric dissolved organic matter, Annu. Rev. Mar. Sci., 5, 447–476, doi:10.1146/annurev-marine-120710-100751, 2013.

BGD
12, 7209–7255, 2015

Nelson, N. B., Siegel, D. A., and Steinberg, D. K.: Production of dissolved organic matter by Sargasso Sea microbes, Mar. Chem., 89, 273–287, doi:10.1016/j.marchem.2004.02.017, 2004.
Nelson, N. B., Siegel, D. A., Carlson, C. A., Swan, C. M., Smethie, W. M., and Khatiwala, S.: Hydrography of chromophoric dissolved organic matter in the North Atlantic, Deep-Sea Res. Pt. I, 54, 710–731, doi:10.1016/j.dsr.2007.02.006, 2007.
Ogawa, H., Amagai, Y., Koike, I., Kaiser, K., and Benner, R.: Production of refractory dissolved organic matter by bacteria, Science, 292, 917–920, 2001.
Organelli, E., Bricaud, A., Antoine, D., and Matsuoka, A.: Seasonal dynamics of light absorption by chromophoric dissolved organic matter (CDOM) in the NW Mediterranean Sea (BOUSSOLE site), Deep-Sea Res. Pt. I, 91, 72–85, doi:10.1016/j.dsr.2014.05.003, 2014.
Parsons, T. R., Maita, Y., and Lalli, C. M.: A Manual of Chemical and Biological Methods for Seawater Analysis, Pergamon Press, Oxford, UK, 173 pp., 1984.
Pavlov, A. K., Silyakova, A., Granskog, M. A., Bellerby, R. G. J., Engel, A., Schulz, K. G., and Brussaard, C. P. D.: Marine CDOM accumulation during a coastal Arctic mesocosm experiment: no response to elevated levels, J. Geophys. Res.-Biogeo., 119, 1216–1230, doi:10.1002/2013JG002587, 2014.
Redfield, A. C.: The biological control of chemical factors in the environment, Am. Sci., 46, 205–221, 1958.
Rochelle-Newall, E. J. and Fisher, T. R.: Production of chromophoric dissolved organic matter fluorescence in marine and estuarine environments: an investigation into the role of phytoplankton, Mar. Chem., 77, 7–21, 2002.
Rochelle-Newall, E. J., Hulot, F. D., Janeau, J. L., and Merroune, A.: CDOM fluorescence as a proxy of DOC concentration in natural waters: a comparison of four contrasting tropical systems, Environ. Monit. Assess., 186, 589–596, doi:10.1007/s10661-013-3401-2, 2014.
Romera-Castillo, C., Sarmento, H., Álvarez-Salgado, X. A., Gasol, J. M., and Marrase, C.: Production of chromophoric dissolved organic matter by marine phytoplankton, Limnol. Oceanogr., 55, 446–454, 2010.
Sugimura, Y. and Suzuki, Y.: A high-temperature catalytic oxidation method for the determination of non-volatile dissolved organic carbon in seawater by direct injection of a liquid sample, Mar. Chem., 24, 105–131, 1988.
Stedmon, C. A. and Álvarez-Salgado, X. A.: Shedding light on a black box: UV-visible spectroscopic characterization of marine dissolved organic matter, in: Microbial Carbon Pump,

BGD
12, 7209–7255, 2015

edited by: Jiao, N. and Azam, F., Senders, The American Association for the Advancement of Science, 62–63, USA, 2011.
Stedmon, C. A. and Bro, R.: Characterizing dissolved organic matter fluorescence with parallel factor analysis: a tutorial, Limnol. Oceanogr.-Meth., 6, 572–579, doi:10.4319/lom.2008.6.572, 2008.
Stedmon, C. A. and Markager, S.: The optics of chromophoric dissolved organic matter (CDOM) in the Greenland Sea: an algorithm for differentiation between marine and terrestrially derived organic matter, Limnol. Oceanogr., 46, 2087–2093, 2001.
Stedmon, C. A. and Markager, S.: Tracing the production and degradation of autochtonous fractions of dissolved organic matter by fluorescence analysis, Limnol. Oceanogr., 50, 1415–1426, 2005.
Stedmon, C. A. and Nelson, N.: The optical properties of DOM in the ocean, in: Biogeochemistry of Marine Dissolved Organic Matter, 2nd edn., edited by: Hansell, D. A. and Carlson, C. A., Elsevier, Eastbourne, UK, 481–508, 2015
Stedmon, C. A., Amon, R. M. W., Rinehart, A. J., and Walker, S. A.: The supply and characteristics of colored dissolved organic matter (CDOM) in the Arctic Ocean: Pan Arctic trends and differences, Mar. Chem., 124, 108–118, 2011.
Strous, M., Pelletier, E., Mangenot, S., Rattei, T., Lehner, A., Taylor, M. W., Horn, M., Daims, H., Bartol-Mavel, D., Wincker, P., Barbe, V., Fonknechten, N., Vallenet, D., Segurens, B., Schenowitz-Truong, C., Médigue, C., Collingro, A., Snel, B., Dutilh, B. E., Op den Camp, H. J. M., van der Drift, C., Cirpus, I., van de Pas-Schoonen, K. T., Harhangi, H. R., Lan Niftrik, L., Schmid, M., Keltjens, J., van de Vossenberg, J., Kartal, B., Meier, H., Frishman, D., Huynen, M. A., Mewes, H.-W., Weissenbach, J., Jetten, M. S. M., Wagner, M., and Le Paslier, D.: Deciphering the evolution and metabolism of an anammox bacterium from a community genome, Nature, 440, 790–794, doi:10.1038/nature04647, 2006.
Sulzberger, B. and Durisch-Kaiser, E.: Chemical characterization of dissolved organic matter (DOM): a prerequisite for understanding UV-induced changes of DOM absorption properties and bioavailability, Aquat. Sci., 71, 104–126, doi:10.1007/s00027-008-8082-5, 2009.
Swan, C. M., Siegel, D. A., Nelson, N. B., Carlson, C. A., and Nasir, E.: Biogeochemical and hydrographic controls on chromophoric dissolved organic matter distribution in the Pacific Ocean, Deep-Sea Res. Pt. I, 56, 2172–2192, doi:10.1016/j.dsr.2009.09.002, 2009.

BGD
12, 7209–7255, 2015

Swan, C. M., Nelson, N. B., Siegel, D. A., and Fields, E. A.: A model for remote estimation of ultraviolet absorption by chromophoric dissolved organic matter based on global distribution of spectral slope, Remote Sens. Environ., 136, 277–285, doi:10.1016/j.rse.2013.05.009, 2013.

Twardowski, M. S., Boss, E., Sullivan, J. M., and Donaghay, P. L.: Modeling the spectral shape of absorbing chromophoric dissolved organic matter, Mar. Chem., 89, 69–88, doi:10.1016/j.marchem.2004.02.008, 2004.

Yamashita, Y., Jaffe, R., Maie, N., and Tanoue, E.: Assessing the dynamics of dissolved organic matter (DOM) in coastal environments by excitation emission matrix fluorescence and parallel-factor analysis (EEM-PARAFAC), Limnol. Oceanogr., 53, 1900–1908, 2008.

Yamashita, Y., Cory, R. M., Nishioka, J., Kuma, K., Tanoue, E., and Jaffé, R.: Fluorescence characteristics of dissolved organic matter in the deep waters of Okhotsk Sea and northwestern North Pacific Ocean, Deep-Sea Res. Pt. II, 57, 1478–1485, doi:10.1016/j.dsr2.2010.02.016, 2010.

Zhang, Y., van Dijk, M. A., Liu, M., Zhu, G., and Qin, B.: The contribution of phytoplankton degradation to chromophoric dissolved organic matter (CDOM) in eutrophic shallow lakes: field and experimental evidence, Water Res., 43, 4685–4697, doi:10.1016/j.watres.2009.07.024, 2009.

Zepp, R. G., Shank, G. C., Stabenau, E., Patterson, K. W., Cyterski, M. J., Fisher, W. S., Bartels, E., and Anderson, S. L.: Spatial and temporal variability of solar ultraviolet exposure of coral assemblages in the Florida Keys: importance of colored dissolved organic matter, Limnol. Oceanogr., 53, 1909–1922, 2008.

BGD
12, 7209–7255, 2015

Table 1. Varied P and Varied N: target concentrations and measured concentrations of DIN and DIN and treatment identifications according to target nutrients concentrations.

Mesocosm ID	Varied P					Varied N				
	target		Measured		Treatment	target		measured		Treatment
	DIN	DIP	DIN	DIP		DIN	DIP	DIN	DIP	
1	12.00	0.75	11.52	0.73	12.00N/0.75P	12.00	0.75	12.58	0.47	12.00N/0.75P
2	12.00	0.75	10.97	0.68	12.00N/0.75P	12.00	0.75	12.36	0.51	12.00N/0.75P
3	12.00	0.75	10.63	0.52	12.00N/0.75P	12.00	0.75	12.61	0.51	12.00N/0.75P
4	6.35	1.10	5.65	1.00	6.35N/1.10P	6.35	0.40	6.91	0.18	6.35N/0.40P
5	–	–	–	–	–	17.65	1.10	18.43	0.79	17.65N/1.10P
6	12.00	1.25	10.74	1.14	12.00N/1.25P	20.00	0.75	20.56	0.47	20.00N/0.75P
7	12.00	1.25	11.16	1.12	12.00N/1.25P	20.00	0.75	20.60	0.45	20.00N/0.75P
8	12.00	1.25	10.89	1.09	12.00N/1.25P	20.00	0.75	21.90	0.45	20.00N/0.75P
9	12.00	1.75	10.55	1.56	12.00N/1.75P	4.00	0.75	4.62	0.44	4.00N/0.75P
10	12.00	0.75	10.82	0.61	12.00N/0.75P	17.65	0.40	18.47	0.22	17.65N/0.40P
11	12.00	1.75	10.82	1.58	12.00N/1.75P	4.00	0.75	4.49	0.47	4.00N/0.75P
12	12.00	1.75	11.07	1.53	12.00N/1.75P	4.00	0.75	3.99	0.49	4.00N/0.75P
13	12.00	0.25	11.16	0.14	12.00N/0.25P	2.00	0.75	2.06	0.46	2.00N/0.75P
14	12.00	0.25	11.18	0.16	12.00N/0.25P	6.35	1.10	6.69	0.78	6.35N/1.10P
15	17.65	1.10	16.90	1.01	17.65N/1.10P	2.00	0.75	1.87	0.56	2.00N/0.75P
16	12.00	0.25	11.33	0.15	12.00N/0.25P	2.00	0.75	2.71	0.4841	2.00N/0.75P

BGD
12, 7209–7255, 2015

Table 2. Estimated linear trends for spectral slope parameters for replicated treatments.

Parameter	Varied P				Varied N			
	12.00N/0.25P	12.00N/0.75P	12.00N/1.25P	12.00N/1.75P	2.00N/0.75P	4.00N/0.75P	12.00N/0.75P	20.00N/0.75P
$S_{275-295}$ (d^{-1} nm^{-1})	-2.3×10^{-3}	-3.2×10^{-3}	-4.0×10^{-3}	-3.0×10^{-3}	-1.4×10^{-3}	-2.3×10^{-3}	-3.2×10^{-3}	-3.3×10^{-3}
S_{SEMO} (d^{-1} nm^{-1})	-0.7×10^{-3}	-1.1×10^{-3}	-1.5×10^{-3}	-1.4×10^{-3}	-1.1×10^{-3}	-1.5×10^{-3}	-2.0×10^{-3}	-2.0×10^{-3}

BGD
12, 7209–7255, 2015

Table 3. Spectral characteristics of excitation and emission maxima and range of intensities (Fmax range) of the three fluorescent components identified by PARAFAC modelling in this study and their comparison with previously reported ones.

this study Peak (region)	Excitation max	Emission max	Fmax range (RU)	Literature Peak (region)	Autor	Properties
Comp.1	235	440–460 (300)	0.0090–0.0450	1 (< 240(355)/476)	Stedmon and Markager (2005)	Humic-like; Accumulated in P- and Si-limited bags Source: Microbial degradation, Sink: Photodegradation
				A (230–260/380–460)	Coble (1996)	humic-, fulvik-like; Source: autochtonous, allochtonous; terrestrial
				C3 (250(310)/400)	Kowalczuk et al. (2009)	Source: Bacterial reworking
				C3 (255(330)/412)	Zhang et al. (2009)	Terrestrial and marine humic-like; Source: microbial activity
				1(< 230–260/400–500)	Ishii et al. (2012)	Small-sized molecules, Photoresistant, biologically unavailible, conservative tracer; Source: Photodegradation
Comp.2	< 230(275)	340	0.0200–0.1305	6 (280/338)	Stedmon and Markager (2005)	Protein-like; Tryptophan-like fluorescence of protenacious material Source: algae at the growth; Sink: UV, microbial reworking
				T (275/340)	Coble (2007)	Tryptophan-like, protein-like; autochtonous
				peak-*T* (275/358)	Romera-Castillo et al. (2010)	protein-like; Source: sterile algae
Comp.3	265	290–300	0.0004–0.2105	4(275/306(338))	Stedmon and Markager (2005)	Protein-like: fluorescence of tryptophan and tyrosine in peptides Higher production rates during establishing algal bloom Source: growing algae Sink: aggregation or microbial uptake
				B (275/305)	Coble 2007	Tyrosine-like, protein-like; Source: autochtonous
				C2 (275/< 300)	Zhang et al. (2009)	Tyrosine-like, protein-like; Source: autochtonous
				7 (270/299)	Yamashita et al. (2008)	Tyrosine-like, protein-like; Source: autochtonous

BGD
12, 7209–7255, 2015

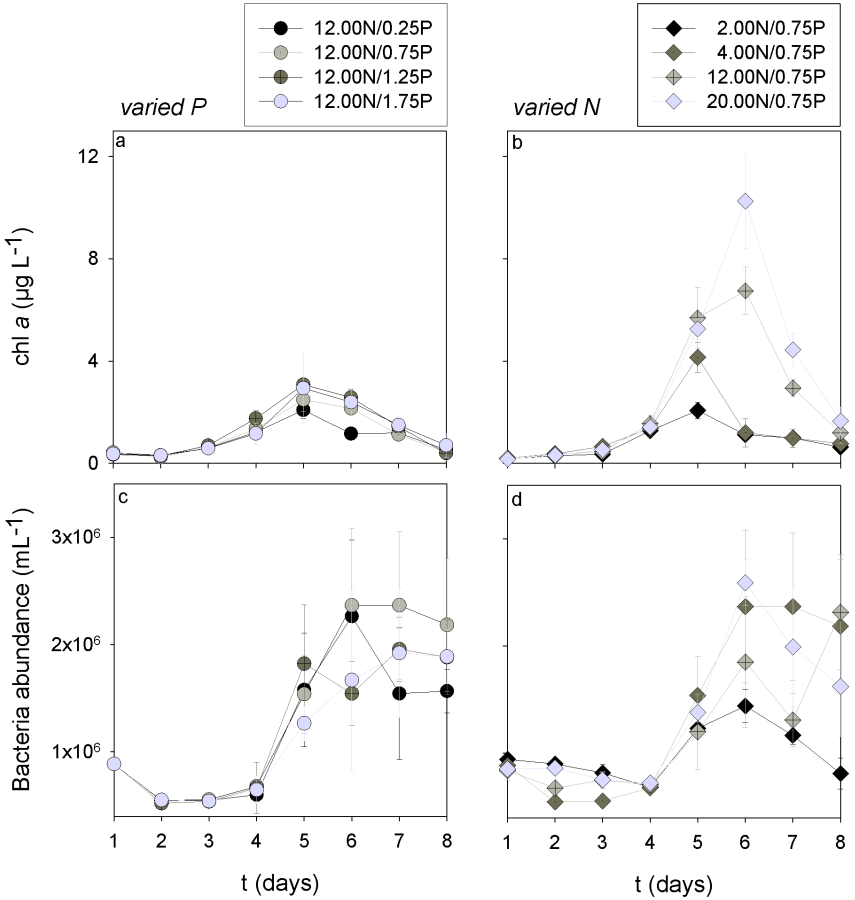

Figure 1. The mean development of chl *a* **(a)**, bacterial abundance **(c)** in replicated treatments during Varied P; and chl *a* **(b)**, bacterial abundance **(d)** in replicated treatments during Varied N.

BGD
12, 7209–7255, 2015

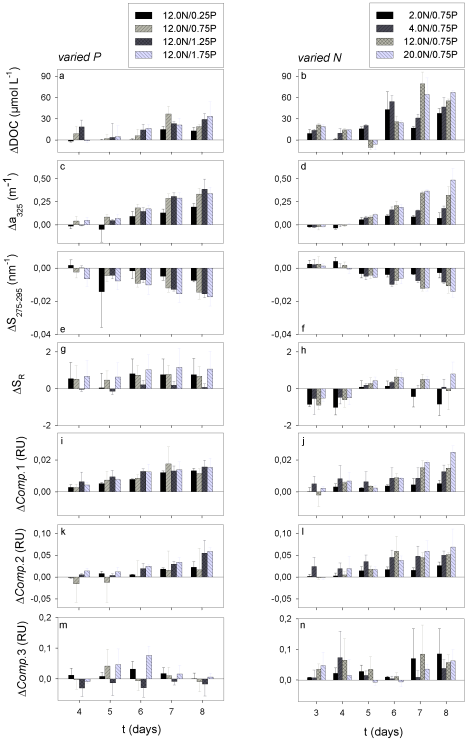

Figure 2. The accumulation over time: of DOC (ΔDOC) **(a)** during the Varied P and **(b)** during the Varied N, of CDOM at 325 nm (Δa_{325}) **(c)** during the Varied P and **(d)** during the Varied N, of Spectral Slope within 275–295 nm spectral range ($\Delta S_{275–295}$) **(e)** during the Varied P and **(f)** during the Varied N, of spectral slope ratio ($S_{275–295}/S_{350–400}$)ΔS_R **(g)** during the Varied P and **(h)** during the Varied N, of first FDOM component fluorescence intensity (ΔComp.1) **(i)** during the Varied P and **(j)** during the Varied N, of second FDOM component fluorescence intensity (ΔComp.2) **(k)** during the Varied P and **(l)** during the Varied N, of third FDOM component fluorescence intensity (ΔComp.3) **(m)** during the Varied P and **(n)** during the Varied N.

BGD
12, 7209–7255, 2015

Effects of nitrate and phosphate supply on chromophoric and fluorescent dissolved organic matter

A. N. Loginova et al.

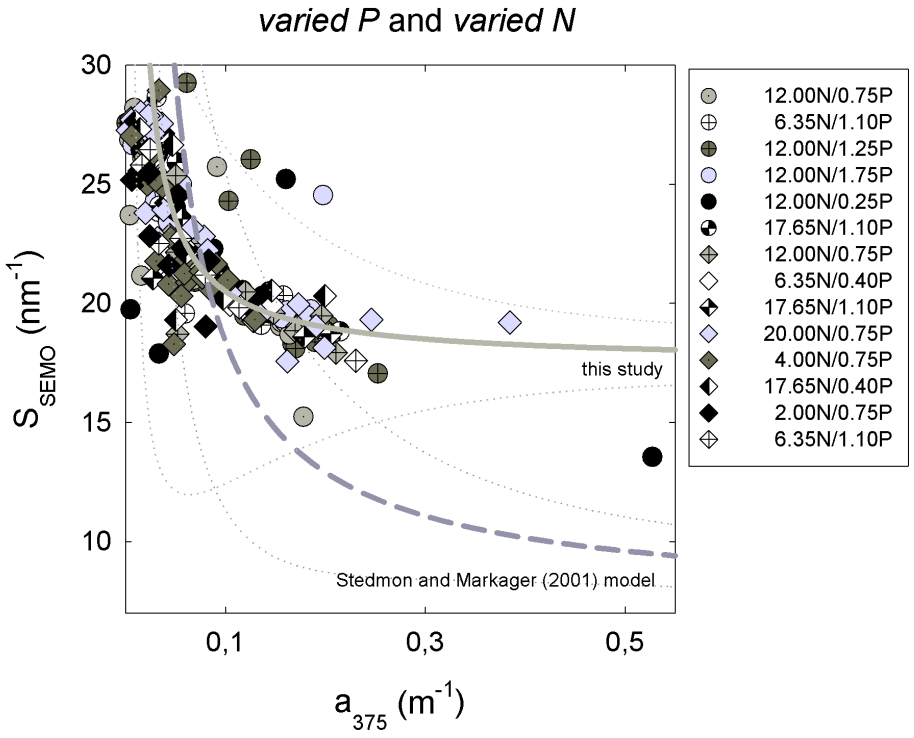

Figure 3. Spectral slope S_{SEMO} against CDOM at 375 nm (a_{375}), obtained during both, Varied P and Varied N experiments (symbols). The dark-grey dashed line is a model of Stedmon and Markager (2001) for marine CDOM with corresponding model limits (dark-grey dotted lines).The reparametrized model, obtained in this study (light-grey line) with model limits (light-grey dotted lines), calculated according to Stedmon and Markager (2001).

BGD
12, 7209–7255, 2015

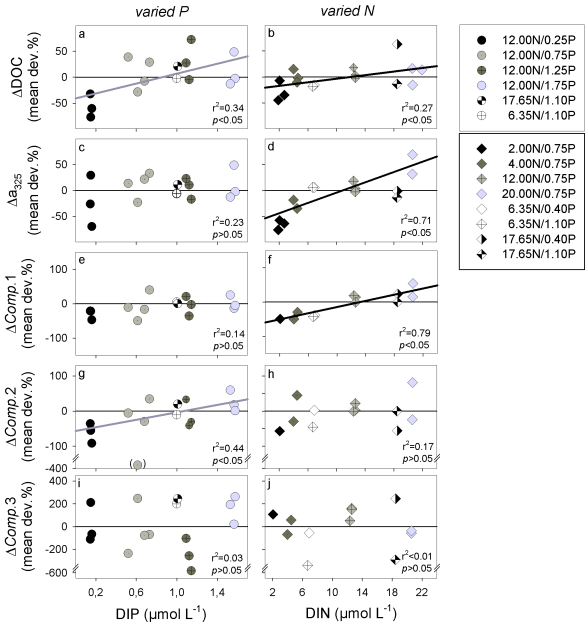

Figure 4. Mean normalized deviations of DOM accumulation against initial nutrients supply. The ΔDOC against DIP initial supply in Varied P **(a)** and against DIN initial supply in Varied N **(b)**, the CDOM absorption at 325 nm (Δa_{325}) against DIP initial supply in Varied P **(c)** and against DIN initial supply in Varied N **(d)**, the first FDOM component intensity (ΔComp.1) against DIP initial supply in Varied P **(e)** and against DIN initial supply in Varied N **(f)**, the second FDOM component intensity (ΔComp.2) against DIP initial supply in Varied P **(g)** and against DIN initial supply in Varied N **(h)** and the third FDOM component intensity (ΔComp.3) against DIP initial supply in Varied P **(i)** and against DIN initial supply in Varied N **(j)** are shown as dashed symbols. The linear regressions are shown by thick light-grey lines in Varied P and by thick black lines in Varied N for those DOM parameters, where covariance with initial nutrients supply was significant. The symbol in brackets in **(g)** was was considered as an outlier and excluded from linear regression analysis.

BGD
12, 7209–7255, 2015

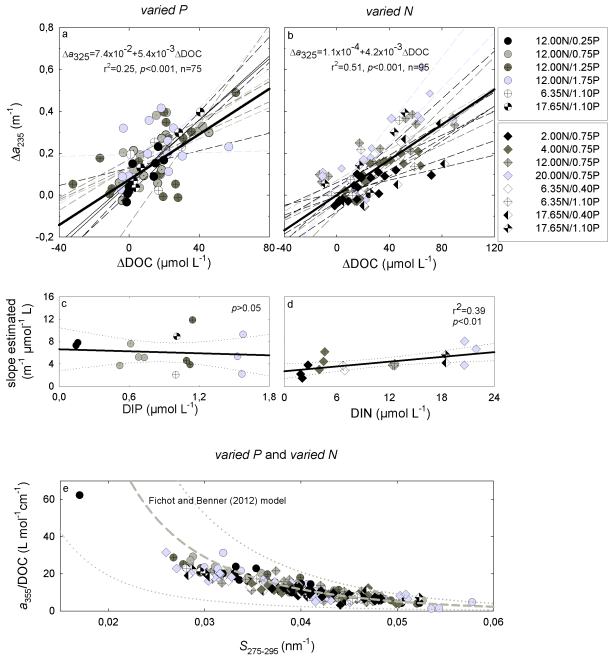

Figure 5. Regression plots of ΔDOC against ΔCDOM at 325 nm **(a)** during Varied P (shaded circles) and **(b)** during Varied N (shaded diamonds). The regression lines for each mesocosm are shown in dashed lines; thick black lines are regressions for all data from Varied P and Varied N respectively. The estimated slopes, of regressions for each mesocosm from **(a, b)** are plotted as *shaded circles* for Varied P **(c)** and *shaded diamonds* for Varied N. The thick black line is the linear regression line with 95 % confidence interval (thin dotted lines). The slope estimated covariance in "Varied N" **(b)** to DIN initial supply can be expressed as: slope estimated = $2.7 \times 10^{-3} + 0.14 \times 10^{-3}$DIN. A spectral slope $S_{275–295}$ against CDOM at 355 nm (a_{355}) for all mesocosms from both experiments are shown as dashed symbols **(e)**, the light-grey dashed line is the model of Fichot and Benner (2012) for DOC calculation with 8 % of uncertainty in a_{355}/DOC indicated by Fichot and Benner (2012) (light-grey dotted lines).

BGD
12, 7209–7255, 2015